The Tropopause Inversion Layer: New Observations, New Theories

Neil F. Tandon[1] (nft2104@columbia.edu), William J. Randel[2], Laura L. Pan[2], Seok-Woo Son[3], Lorenzo M. Polvani[1]

[1]Columbia University, New York, NY, USA; [2]National Center for Atmospheric Research, Boulder, CO, USA; [3]McGill University, Montreal, Quebec, Canada

Abstract

There is now great interest in the tropopause inversion inversion layer (TIL), a 1-2 km region just above the tropopause where there is a spike in static stability. Radio occultation data from the COSMIC GPS mission are providing an unprecedented level of spatial and temporal resolution with which to analyze the TIL. We start by showing the agreement between GPS data and radiosondes. We then examine the causes and consequences of the TIL. Observations from the ACE satellite and fixed dynamical heating calculations suggest strong roles for water vapor and ozone in the formation and modulation of the TIL. This agrees with observations showing a large TIL in the polar summer, where water vapor levels are persistently high. It is also clear that TIL strength is related to vorticity, but observations and models have important differences that need to be reconciled. These dynamical considerations dovetail with observations showing high TIL variability in the storm-track regions. Finally there is evidence from ozonesonde data that the TIL may be coupled to transport across the tropopause.

Data

+ COSMIC GPS radio occultation data, 2006-2009. 200m vertical resolution..
+ Radiosonde data from the IGRA database, 1980-2009. Mandatory levels and tropopause levels were used. Cubic interpolation was applied when calculating static stability.
+ NCEP/NCAR reanalysis, 1980-2009. Mandatory levels and tropopause level were used. Cubic interpolation was applied when calculating static stability.
+ ACE Satellite data, 2004-2009.
+ Ozonesonde data, 2000-2009. 27 stations from 30N-90N. 200m vertical resolution.
+ Global Forecasting System (GFS), April 4, 2008.

What is the TIL?

+ The TIL is the region 0-1km above the tropopause where there is often a spike in static stability.
+ To make sense of the TIL, it is useful to examine some sample soundings.
+ The spike in static stability coincides with a negative spike in temperature.
+ The TIL also coincides with a large potential temperature lapse rate.

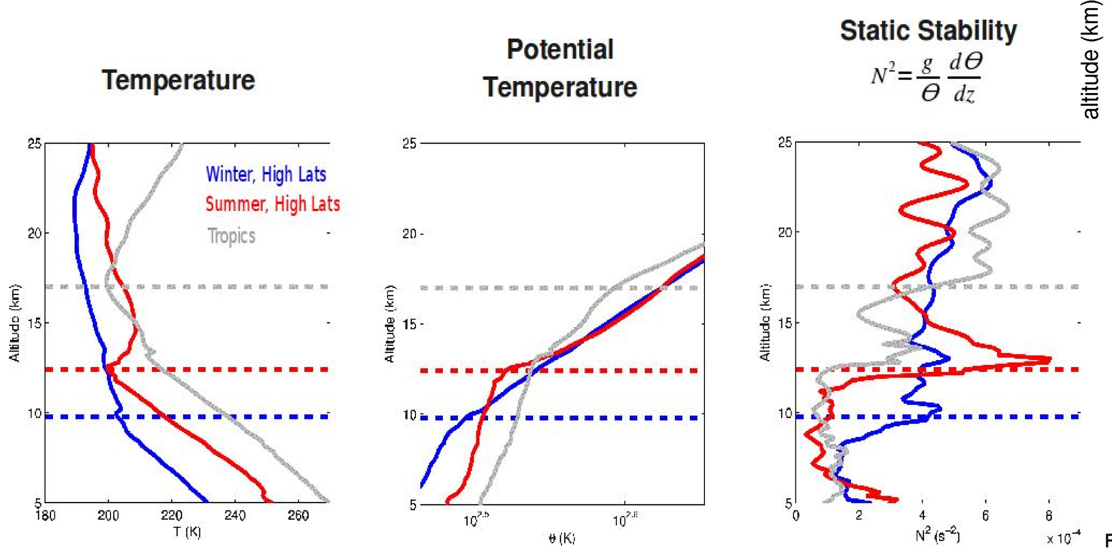

Figure 1. Example soundings from COSMIC GPS data. The dotted line indicates the lapse rate tropopause. The blue sounding is from DJF NH high latitudes, the red from JJA NH high latitudes, and the gray from the tropics.

Definitions

N^2 is the static stability, defined by $N^2 = g/\theta\ d\theta/dz$.

N^2_{TIL} is the average static stability in the TIL. For COSMIC and radiosondes, the TIL is taken to be 0-1km above the tropopause. For NCEP the TIL is taken to be 1-2km above the tropopause. The reasons for these conventions is explained below.

Zonal Structure

+ There is a strong TIL in the summer high latitudes.
+ There is a pronounced TIL in the winter midlatitudes.
+ The TIL in NCEP (not shown) actually appears higher and weaker than in COSMIC and radiosondes. This may be due to the way satellite data is assimilated in NCEP (Birner 2006). For this reason, we have defined N^2_{TIL} differently for NCEP, as mentioned above.

RESULT: With the increased vertical resolution from COSMIC, we now observe a TIL in the tropics during JJA. This is not visible with low resolution data.

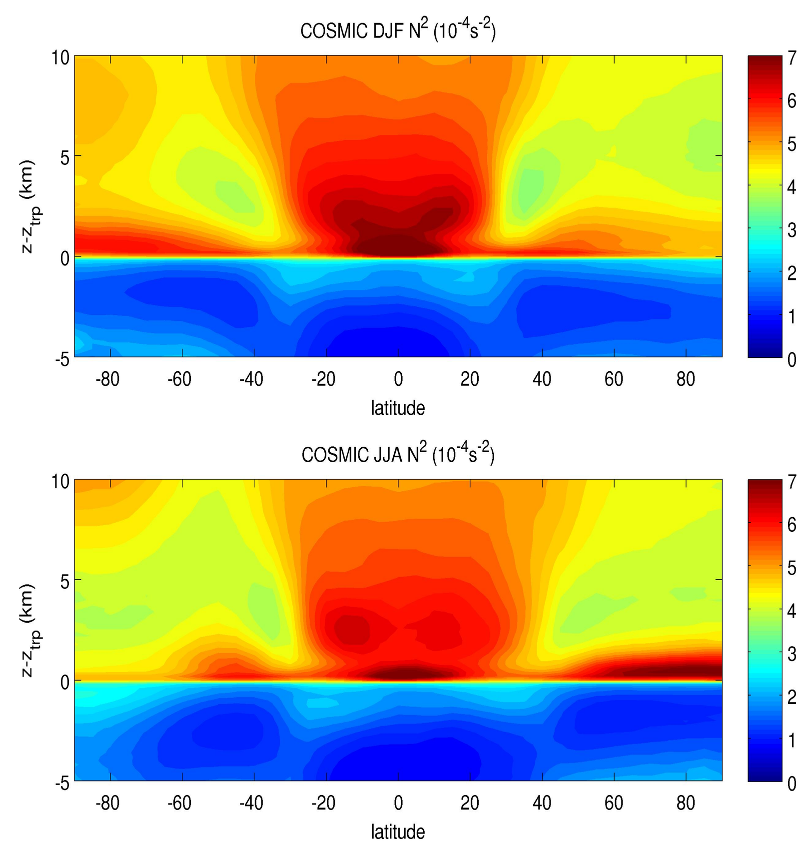

Figure 2. Zonally averaged static stability from COSMIC GPS data. Averaging was performed in tropopause-based coordinates. The contour interval is 0.2×10^{-4} s^{-2}. The seasonal averages for DJF (top) and JJA (bottom) are shown.

Radiation and the TIL

+ The radiative balance of ozone, carbon dioxide and water vapor can produce a TIL (Manabe & Strickler 1964).
+ We obtained water vapor climatology from the ACE satellite. We then performed a fixed dynamical heating (FDH) calculation using NCAR's single column model.

RESULT: Figure 3 suggests that water vapor can be strongly coupled to TIL strength.

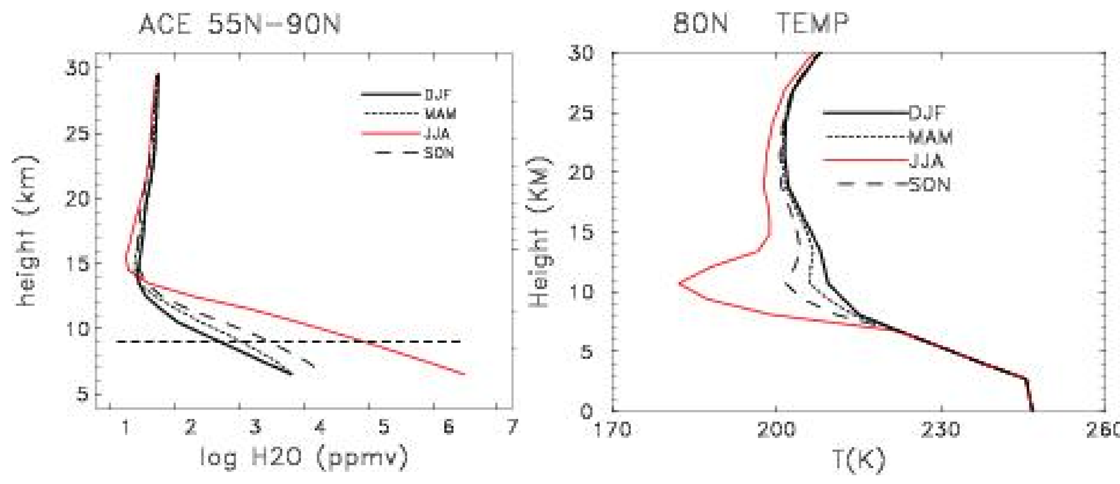

Figure 3. Left, seasonal climatology of water vapor mixing ratio in the NH polar region. Data were obtained from from the ACE satellite. These water vapor values were then used in the NCAR single column model to determine the temperature profile (right).

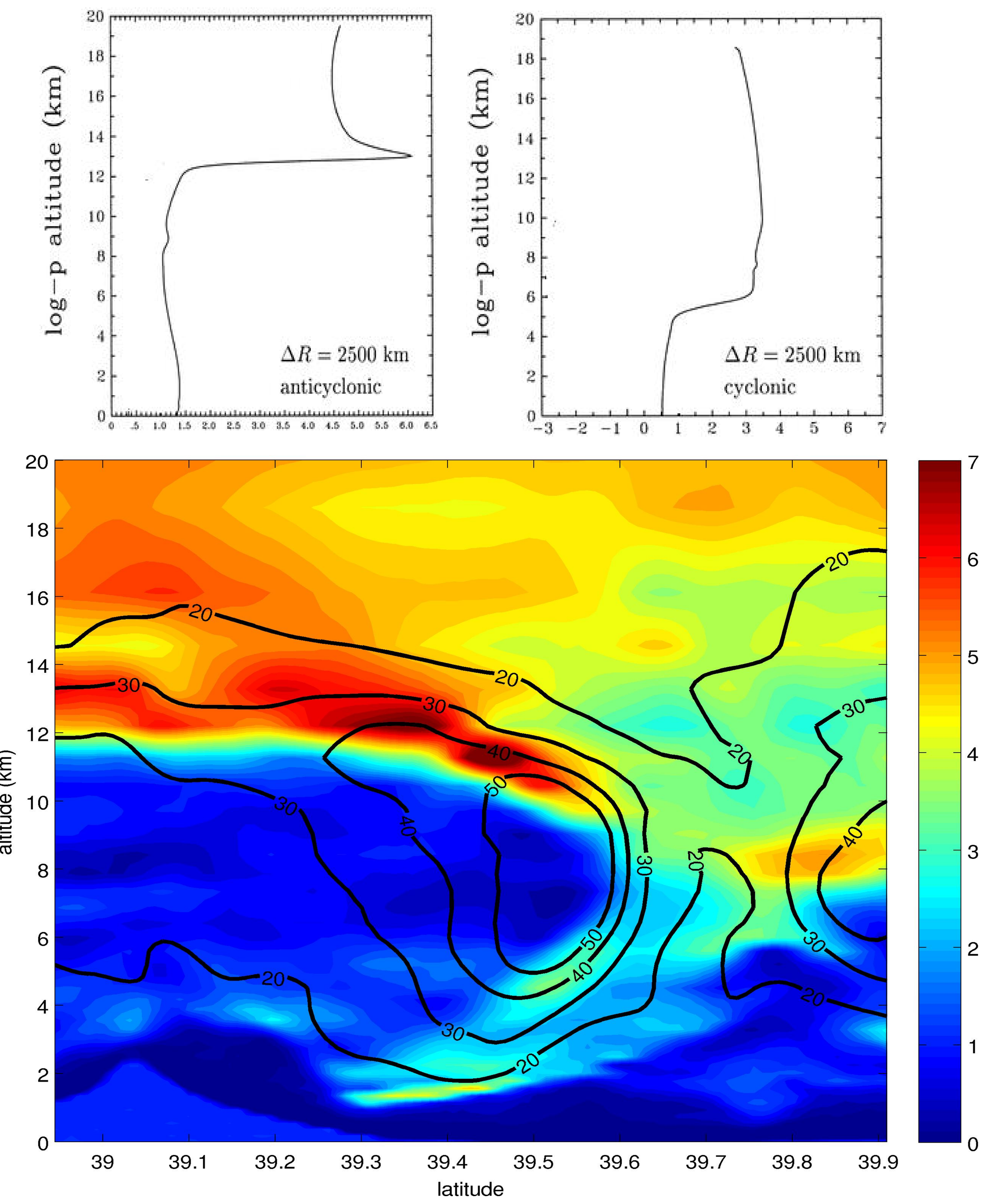

Figure 4. Top are profiles of static stability calculated by Wirth (2003) for anticyclonic vorticity (left) and cyclonic vorticity (right). Bottom is a vertical slice from GFS data, April 4, 2008. The filled contours are static stability, with a contour interval of 0.2×10^{-4} s^{-2}. The line contours are wind speed in m/s.

Dynamics and the TIL

+ Wirth (2003) and Son & Polvani (2007) showed that a TIL can be generated from dynamics alone.
+ Wirth (2003) showed from simulations that in a strongly cyclonic vortex, there is no TIL, while in a strongly anticylclonic vortex there is a strong TIL.
+ Son & Polvani (2007) showed from simulations that, with certain forcings, a TIL can exist even in a cyclonic vortex.
+ Randel (2007) showed from observations and reanalysis that there is a TIL in cyclonic vortices,
+ Using GFS, we have obtained an instantaneous picture of static stability around a jet core (Figure 4)

RESULTS:

+ Figure 4 clearly shows that on the cyclonic (north) side of the jet, there is no TIL, while on the anticyclonic (south) side of the jet there is a strong TIL. This is consistent with Wirth (2003).
+ It is also clear that this region of no TIL is very confined. So coarse spatial averaging will likely show a TIL even in cyclonic vortices. This may explain the difference with Randel (2007). Of course, Figure 4, bottom, is just one instance, so more detailed observations are still needed.

Spatial Structure

+ We plotted N^2_{TIL} for COSMIC, IGRA, and NCEP.

RESULTS:

+ There is good overall agreement between COSMIC and IGRA. NCEP shows weaker TIL and different spatial structure.
+ The length of the COSMIC record is shorter, but there is good agreement with radiosondes nonetheless.
+ There is a strong TIL over the winter storm tracks. In the NH winter, there are pronounced peaks over the eastern Pacific and eastern Atlantic. NCEP smears out this storm track signature.
+ There is a strong TIL in the summer high latitudes. There is a slight asymmetry between NH and SH.

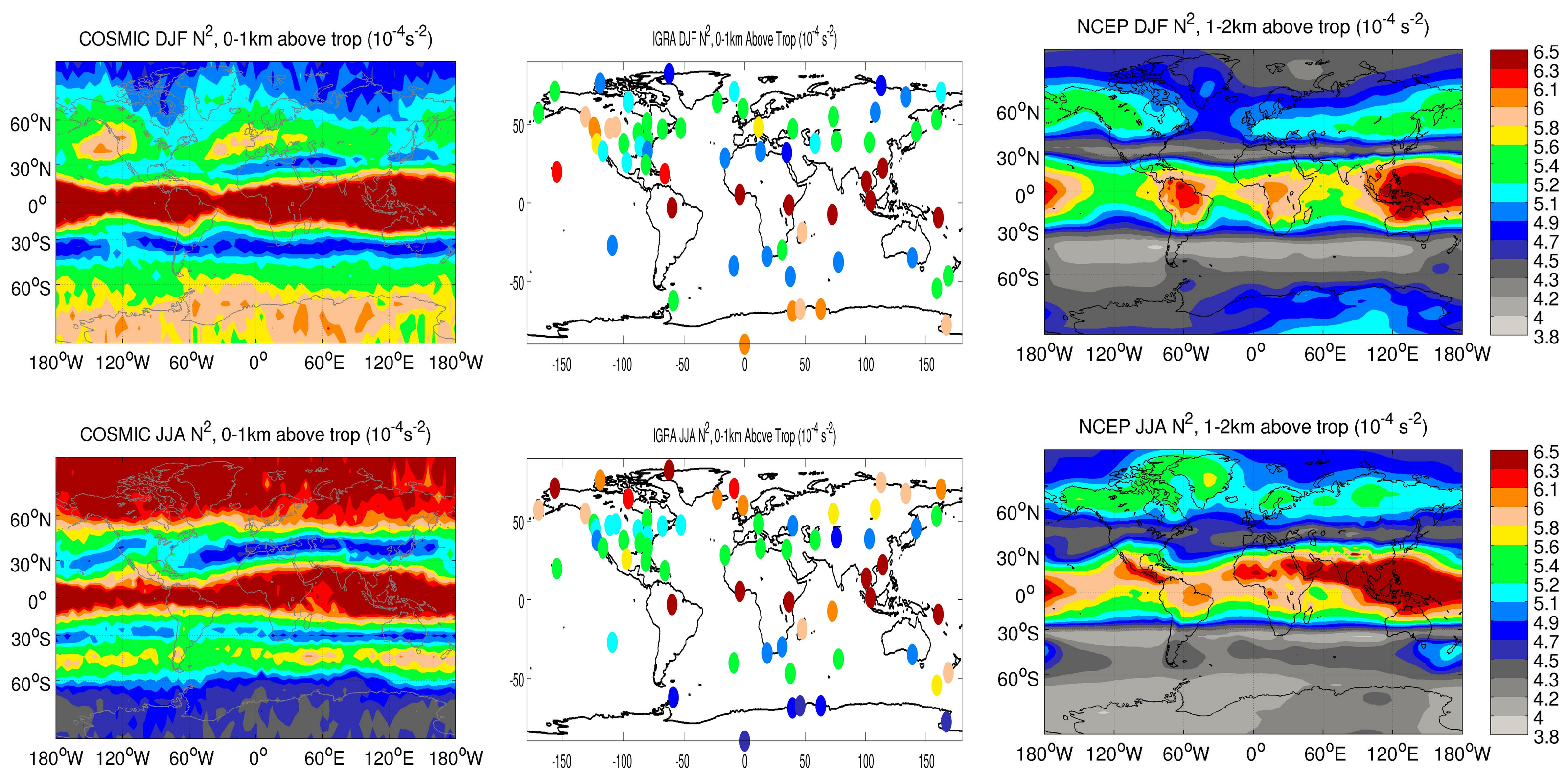

Figure 5. The average static stability in the TIL. Data are derived from COSMIC GPS (left), radiosondes (middle) and NCEP/NCAR reanalysis (right). Seasonal averages were taken for DJF (top row) and JJA (bottom row).

Variability

+ We calculated the standard deviation of N^2_{TIL} for the three datasets.

RESULTS:

+ COSMIC and IGRA are in good agreement.
+ Strongest variability is seen over the tropics and winter storm tracks.
+ Variability in the winter storm tracks suggests that synoptic scale eddies are responsible for TIL formation.
+ Low variability in the polar summers suggests that slower radiative processes are the dominant contributer.

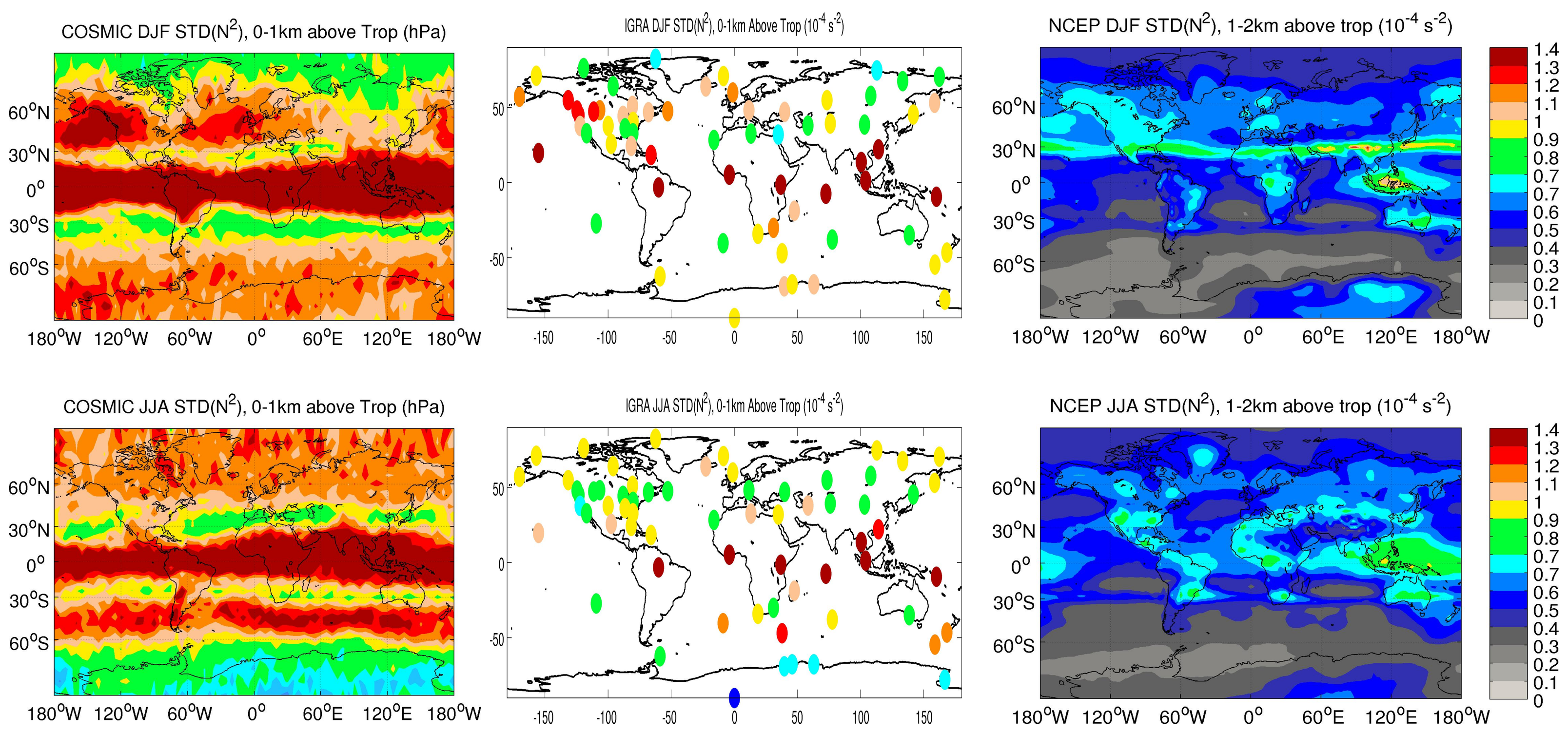

Figure 6. The standard deviation of TIL static stability for COSMIC (left), radiosondes (middle), and NCEP (right). DJF values are in the top row, JJA the bottom row.

The TIL and Transport

+ We considered how the TIL may impact transport across the tropopause.
+ Ozone is a reliable tracer for stratospheric air.
+ If stratospheric and tropospheric air are well separated, then there will be a sharp discontinuity in the ozone profile across the tropopause.
+ Using ozonesonde data in the NH extratropics, we plotted ozone profiles for strong TIL cases and profiles for weak TIL cases,

RESULT: We see that when there is a strong TIL, there is a sharper separation between stratospheric and tropospheric air.

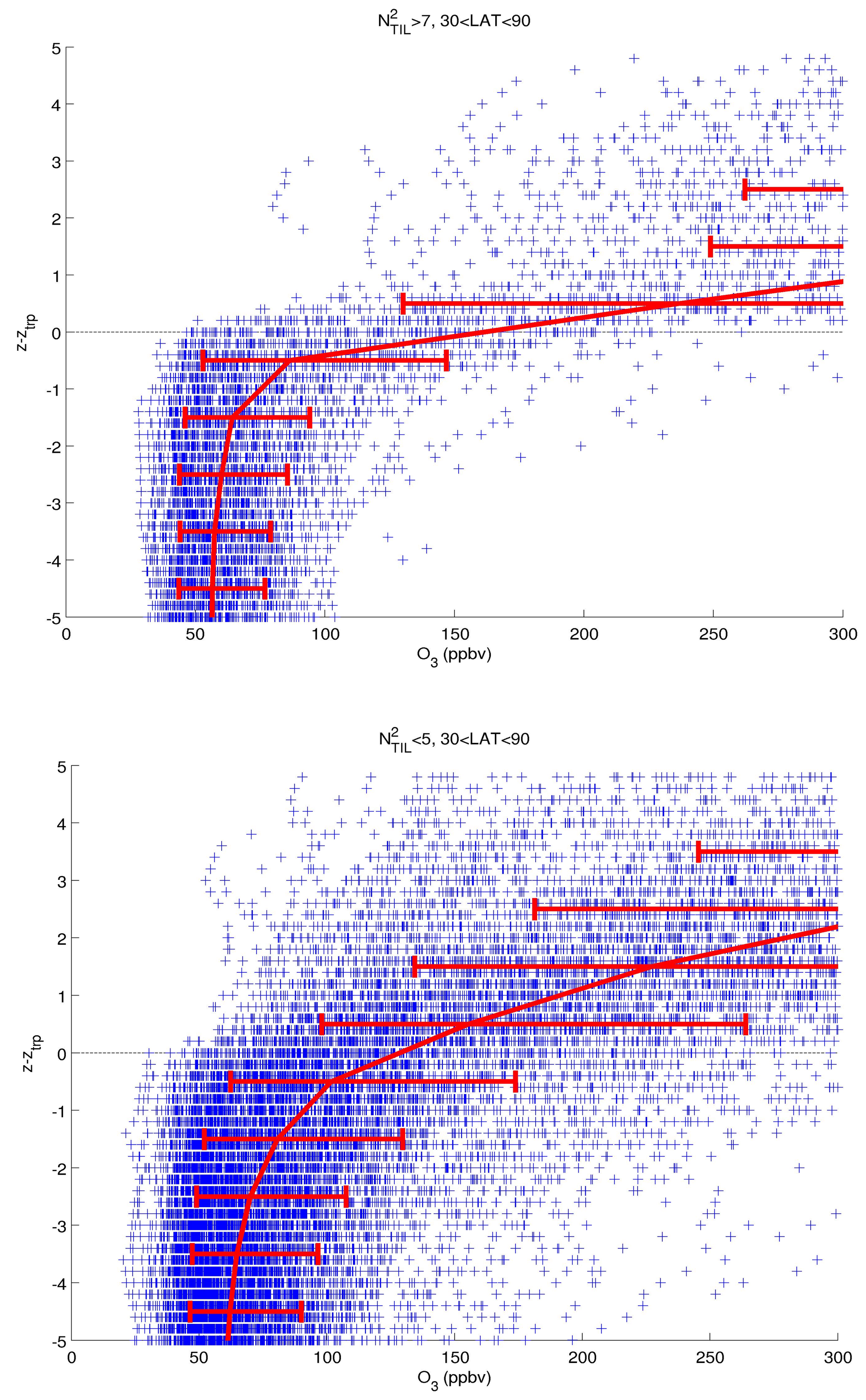

Figure 7. Ozone profiles derived from ozonesondes in the 30-90N region. The profiles are sorted into those with $N^2_{TIL}>7\times10^{-4}$ s^{-2} (top) and those with $N^2_{TIL}<5\times10^{-4}$ s^{-2} (bottom). The profiles are plotted in tropopause-based coordinates. The red line indicates the median for each 1km bin, and the errorbars span the 70th percentile.

References

Birner, T., D. Sankey, and T. G. Shepherd (2006), The tropopause inversion layer in models and analyses, **Geophys. Res. Lett.**, 33, L14804, doi:10.1029/2006GL026549

Manabe, S., and R. F. Strickler, 1964: Thermal equilibrium of the atmosphere with a convective adjustment. **J. Atmos. Sci.**, 21, 361-385.

Randel, W.J., F. Wu, and P. Forster, 2007: The extratropical tropopause inversion layer: global observations with GPS data, and a radiative forcing mechanism. **J. Atmos. Sci.**, 64, 4489–4496.

Son, S.-W., and L. M. Polvani (2007), Dynamical formation of an extra-tropical tropopause inversion layer in a relatively simple general circulation model, **Geophys. Res. Lett.**, 34, L17806, doi:10.1029/2007GL030564.

Wirth, V., 2003: Static stability in the extratropical tropopause region. **J. Atmos. Sci.**, 60, 1395–1409.